Induced gamma-band activity is related to the time point of object identification

Martinovic, Jasna[1,2]

Gruber, Thomas[1]

Hantsch, Ansgar[1]

and

Müller, Matthias M. [1]

[1] **- Institut für Psychologie I, Universität Leipzig, Germany**

[2] **- School of Psychology, University of Liverpool, UK**

Total number of Pages: 44

Number of Tables: 4

Number of Figures: 7

Corresponding Author:

Matthias Müller
Institut für Psychologie I, Universität Leipzig,
Seeburgstrasse 14-20,
04103 Leipzig,
Germany.
Tel.: +49-341-973 5962
Fax: +49-341-973 5969
Email: m.mueller@rz.uni-leipzig.de

Abstract:

Object recognition is subserved by mechanisms that seem to rely on the activity of distributed neural assemblies coordinated by synchronous firing in the gamma-band range (>20Hz). The present study relied on a novel EEG-compatible plane-rotation paradigm to elicit view-dependent processing leading to delays in the recognition of disoriented objects. The paradigm involved a covert naming task (grammatical gender decision). The task's suitability was first evaluated through a control experiment that contrasted covert with overt naming. The plane-rotation paradigm was subsequently employed in an EEG experiment. It was found that recognition delays for disoriented objects were accompanied by induced gamma-band activity's (GBA) peak latency delays, replicating Martinovic, Gruber and Müller (2007, *Journal of Cognitive Neuroscience*). Brain electrical tomography was performed to obtain further information on the intracranial current density distributions underlying the latency shifts. Induced GBA was found to be generated by a set of distributed prefrontal, temporal and posterior sources committed to representational processing. Their relative contribution differed between upright and disoriented objects, as prefrontal activity became more prominent with increased disorientation. Together these findings indicate that adaptive changes in dynamic coding of object identity occur during recognition of disoriented objects. Induced GBA is a marker of pronounced sensitivity to these changes and thus a robust neural signature of representational activity in high-level vision.

Section: Cognitive and Behavioral Neuroscience

Keywords: gamma-band activity, naming, object identification, view-dependent recognition, EEG, source localisation

1. Introduction

Studies on mechanisms of high-level vision suggest objects are represented through formations of distributed feature-coding neural assemblies. Within and between these assemblies transient integrative activity is thought to occur through synchronous firing in the gamma-band frequencies (> 20 Hz) (Gruber and Müller, 2005; Varela et al., 2001). This type of activity can be detected in the high frequency range (30-90 Hz) of the human electroencephalogram (EEG). It can be either evoked or induced depending on whether it is or is not time- and phase-locked to stimulus onset (Singer and Gray, 1995). In the visual domain it has been repeatedly demonstrated that evoked gamma-band activity (GBA), occurring at approx. 100 ms post-stimulus onset, is related to the processing and integration of features (Busch et al., 2004; Karakas and Basar, 1998). Meanwhile, induced GBA, occurring at approx. 200-400 ms post-stimulus onset, is a signature of cortical object representation (Kaiser et al., 2004; Lachaux et al., 2005; Tallon-Baudry and Bertrand, 1999; Tallon-Baudry et al., 2005); particularly the late representational processing that follows successful identification (Fiebach et al., 2005; Gruber et al., 2004; Gruber and Müller, 2005; Martinovic et al., 2007).

An abundance of evidence shows that increases in induced GBA amplitude accompany successful recognition of complex meaningful objects (Gruber et al., 2004; Gruber and Müller, 2005; Lachaux et al., 2005; Tallon-Baudry et al., 2005). However, its time course has not been successfully related to object identification until a recent study (Martinovic et al., 2007) demonstrated that delays in peak latency of induced GBA accompanied delays in the recognition of disoriented objects. In that study, participants had to covertly name images that could either be presented upright or disoriented in the picture plane. Covert naming was performed in the form of a phonological decision on the first letter

of the object's name, with vowels as rare stimuli. While induced GBA showed latency shifts, evoked GBA and event-related potential (ERP) components remained unmodulated. However, the delays in behavioural and neurophysiological measures of recognition failed to show a direct correlation. It has already been reported that repetition suppression in induced GBA amplitude relates to RT benefits obtained through visual priming, although the two measures do not correlate (e.g., Fiebach et al., 2005). Therefore the authors concluded that the findings provide further evidence in support of the Tallon-Baudry and Bertrand's (1999) representational hypothesis, which claims that induced GBA is a neural marker of object coding.

Martinovic et al.'s (2007) plane-rotation paradigm used a covert naming task in order to elicit delays in the recognition of disoriented objects. Such view-dependent recognition effects are a phenomenon that has long been known in behavioural literature. Picture-plane rotated two-dimensional (2D) images of familiar objects with a predominant environmental orientation (e.g., horse, table, chair, etc.) generally require more time to be *overtly named* than upright images (Jolicoeur, 1985; McMullen and Jolicoeur, 1990; Murray, 1995a). Such orientation effects are observed in speeded naming tasks performed on large and diverse stimulus sets, therefore demanding recognition to employ view-dependent mechanisms (Murray, 1998). *Overt naming* delays for disoriented objects obtained with plane-rotation paradigms are generally considered to reflect delays in recognition processes themselves. These delays are thought to arise due to a nonlinear image normalisation that is needed for the initial identification of the object (Jolicoeur et al., 1998; Lawson and Jolicoeur, 2003; Willems and Wagemans, 2001). An alternative view claims that the viewpoint costs do not occur during intial identification. This account, based on attentional blink and repetition blindness paradigms, claim that costs are incurred when representations become consolidated in visual memoryDux and Harris, 2007; Harris and Dux, 2005). The early versus late

viewpoint-effect distinction from behavioural literature does not challenge Martinovic et al.'s (2007) findings. As induced GBA is related to late representational processing, the delay that is observed in their peak latency could be due to an intervening process at either the initial or the consolidated representation stage.

The aim of the present study was to replicate and extend Martinovic et al.'s (2007) findings on the relatedness of induced GBA to object recognition processes. In relation to Martinovic et al. (2007), the present study introduces three major new elements. First of all, modifications were introduced to the plane-rotation paradigm in order to increase the quality of the data. The assignment of stimuli to the upright and disoriented conditions was counterbalanced across the sample instead of being fixed condition-wise as in Martinovic et al. (2007). Also, a more stringent gender decision task was used instead of the phonological decision that was employed by Martinovic et al. (2007)[1].

Secondly, in order to assess the validity of covert tasks a control experiment was conducted. It contrasted overt and covert naming (i.e. gender decision) in eliciting object recognition delays with a plane-rotation paradigm. Martinovic et al. (2007) implicitly posited that tasks based on covert naming directly correspond to overt naming. However, the comparability between overt and covert naming should be experimentally examined. Convergence of covert and overt RTs would allow us to confidently relate RT delays from covert tasks to the timing of recognition processes.

Lastly, the EEG experiment was more extensive than in Martinovic et al. (2007). In addition to behavioural, ERP and event-related GBA analyses it included brain electrical tomography (BET). This was done in order to ascertain if shifts in latency are also accompanied by changes in the activity of generating cortical structures. A distributed set of prefrontal, temporal and posterior regions, committed to object recognition, were expected to

[1] 'Materials and Procedure' section of the Methods contains information on the importance of stimulus counterbalancing in plane-rotation studies. It also provides the relevant information on the advantages of a grammatical gender decision task.

be the sources of GBA induced by entry-level object recognition (for previous findings using a categorisation task, see Gruber et al., 2006; for a detailed model describing regions involved in object identification, see Bar, 2003). If induced GBA was indeed a marker of dynamic object coding, as Martinovic et al. (2007) proposed in their conclusion, adaptive changes that lead to latency shifts should also be visible from the pattern of activity within these distributed sources. In line with Bar's (2003) model, prefrontal generators should become more prominent with increased rotation through additional or prolonged top-down processing of possible templates that define object identity for disoriented objects (for evidence for such top-down inputs in high-level vision, see Bar et al., 2006). Therefore, it was hypothesised that for disoriented objects prefrontal sources should progressively enhance their activity relative to the temporal and posterior sources.

There is an additional reason for complementing the latency shifts in induced GBA with another independent measure of a change in activity. From a methodological point peak amplitude and latency in the waveforms obtained from EEG signal cannot be considered to be fully independent (Otten and Rugg, 2005). This is due to the fact that latency actually reflects changes in the distribution of amplitude over time and in the presence of jitter it also depends on the differences in variance between conditions. A shift in peak latency without a change in amplitude was interpreted in Martinovic et al. (2007) as a delay which may also reflect a more general change in the distribution of underlying high-frequency oscillatory activity. Therefore looking for shifts in the amount of activity of distributed sources between upright and disoriented objects allows us to get one step closer to the actual change in adaptive neural processing that may be reflected in the induced GBA latency modulations. If such changes in cortical processes were identified, it would allow us to connect induced GBA with specific aspects of late representational processing of objects.

2. Results

2.1. Results of the Control Experiment

In this experiment RTs from a covert naming paradigm (i.e. gender decision) were contrasted to those from overt naming using a plane-rotation paradigm. It was hypothesised that both tasks would produce recognition delays for disoriented objects and that the obtained naming times would correlate with each other suggesting that same processes subserved overt and covert tasks.

Table 1 shows accuracy rates and RTs for overt and covert tasks. Error rate for overt naming was 21.87 ± 2.13 % while missing data amounted to 3.27 ± 0.82 %. In covert naming error rate was 19.35 ± 3.28 % and missing data amounted to 2.20 ± 0.77 %. For overt naming it is possible to differentiate between several types of wrong responses. Wrong names that carry the same gender as the correct response, which would be accepted as an accurate answer in the covert task, amounted to 1.32 ± 0.38 %. Non-dominant names[2] with same gender, which would be classified as wrong in overt but as correct in covert naming, were shown to be quite high at 9.15 ± 1.20 %. Non-dominant names of different gender were at 6.79 ± 1.09 % and wrong names with different gender were at 2.31 ± 0.63 %. Errors due to lipsmacking, disfluency or technical malfunction came to 2.39 ± 0.44 %.

---

insert Table 1 about here

---

[2] Images of objects often have several alternative names. In naming studies, different participants will end up producing different names in response to the stimulus picture. The name that is most often produced is referred to as the 'dominant name' while other less frequent alternatives are called 'non-dominant names'.

As expected, for both overt and covert tasks there were no significant RT differences between 60° and 300° or between 120° and 240° therefore in all further analyses they were averaged together to form two conditions (±60° and ±120° departures from upright).

A 2x3 repeated measures ANOVA (task; degree of rotation) across subjects was performed to contrast the accuracy rates. No main effect for the type of task ($F(2, 22) = 1.22$, n.s.) was found but there was a trend for disorientation ($F(2, 22) = 3.34$, $p = 0.07$). There was no interaction between the factors ($F < 1$). As Table 1 shows, the approaching significant effect of disorientation was mainly due to the fact that for covert naming there is an insignificant tendency for accuracy rates to decrease with increasing disorientation ($F(1, 11) = 3.14$; $p = 0.06$). No such trend was present for overt naming ($F(1, 11) = 1.83$; n.s.).

RT analyses were performed across subjects (2x3 repeated measures ANOVA with factors task and degree of rotation) with disorientation effects further examined across items (one-way ANOVA). Main effects of task ($F(2, 22) = 93.3$, $p < 0.001$) were found. Response latencies were about 200-300 ms longer for gender decision than for overt naming leading to a significant effect. Disorientation resulted in longer response times yielding a significant rotation effect ($F(2, 22) = 8.15$, $p < 0.01$). The interaction between the two factors ($F(2, 22) = 3.08$, $p = 0.07$) approached significance, as differences in response latencies seemed to increase for the disorientation of ±120° (paired *t*-tests: upright (278 ms), $t(11) = 9.13$, $p < 0.001$; ±60° (247 ms), $t(11) = 8.23$, $p < 0.001$; ±120° (338 ms), $t(11) = 7.56$, $p < 0.001$). Main effect of disorientation was found for the gender decision ($F(2, 11) = 12.25$, $p < 0.001$) but not for overt naming ($F(2, 11) = 2.52$; $p=0.12$). This difference arose mainly due to a lack of a RT delay for the ±120° condition in overt naming (paired t-test for ±60° vs. ±120°, $t(11) < 1$). In an across item analysis the effect of rotation on RTs was present for both overt ($F(2,917) = 4.68$; $p < 0.01$) and covert ($F(2,972) = 4.82$; $p < 0.01$) naming. Also, both overt and

covert naming showed that the delay effect was linear when analyses across items were performed (overt: $F(1, 918) = 6.17$, $p < 0.05$; covert: $F(1, 973) = 8.98$; $p < 0.01$).

Post hoc correlational analysis across participants (Pearson coefficient) was carried out to examine the relations between accuracy rates and RTs. Accuracy did not correlate with RTs for either overt ($r = -0.14$, $r = -0.14$, $r = -0.25$, for 0°, ±60° and ±120° respectively; n.s.) or covert naming ($r = 0.38$, $r = 0.37$, $r = 0.43$, for 0°, ±60° and ±120° respectively; n.s.). The absence of correlations between accuracy and RTs indicates there was no speed-accuracy trade-off in either task.

In order to establish a relation between reaction times resulting from overt and covert tasks correlational analyses were carried out both across participants and across items. There were no significant correlations for reaction times across participants between overt and covert tasks ($r = 0.24$, $r = 0.48$, $r = 0.20$, for 0°, ±60° and ±120° respectively; n.s.). Partial correlation across items, controlling for subject pairs, showed a highly significant albeit small correlation ($r = 0.23$, $p < 0.001$).

2.2. Results of the EEG Experiment

2.2.1. Behavioural data

Mean accuracy rate was 85.7 ± 0.8 %. RTs were computed for correctly answered trials between 400 and 2300 ms.

As expected there were no significant RT differences between 60° and 300° or between 120° and 240° therefore they were averaged together to form two conditions (±60° and ±120° departures from upright) in all further analyses. The following recognition RTs were found: 0°, 1162 ± 26 ms; ±60°, 1200 ± 29 ms; ±120°, 1243 ± 27 ms.

Repeated measures ANOVA with the factor CONDITION (0°, ±60° and ±120°) revealed a highly significant overall effect of rotation ($F(2,17) = 17.97$, $p < 0.001$). Post-hoc paired t-tests elucidated the effect was present between all three conditions. Participants responded to ±120° rotated stimuli significantly slower than both upright ($t(17) = -6.16$, $p < 0.001$) and ±60° rotated stimuli ($t(17) = -2.82$, $p < 0.05$). The ±60° rotated stimuli were also responded to more slowly than the upright ones ($t(17) = -3.19$, $p < 0.005$).

Post hoc correlational analysis across participants (Pearson coefficient) found that accuracy did not correlate with RTs ($r = -0.01$, $r = -0.04$, $r = -0.13$, for 0°, ±60° and ±120° respectively; n.s.). The absence of correlations between accuracy and RTs indicates there was no speed-accuracy trade-off.

2.2.2. Event related potentials

Figure 1 depicts the ERPs at anterior regional means as well as parietal and occipital regional means for all three conditions (see Figure 7 for regional means' locations).

---

insert Figure 1 about here

Table 2 provides both the properties of the ERP components and their baseline corrected mean amplitudes averaged across the respective time windows at the site of interest, tested with repeated measurement ANOVAs to compare across the three conditions (0°, ±60° and ±120°).

---

insert Table 2 about here

As Table 2 shows no significant amplitude modulations were found in any of the components (N1, P300, and parietal negativity).

2.2.3. Induced and evoked spectral changes

Figure 2 shows grand mean baseline-corrected time-by-frequency plots (TF-plots) across 18 participants collapsed across all three experimental conditions. Evoked and induced GBA are depicted from a mean across all 128 electrodes.

Table 3 presents results for GBA peak amplitude and peak latency.

---

insert Table 3 about here

---

insert Figure 2 about here

Gamma-band amplitude evoked by picture presentations was enhanced (Figure 2a) at occipital sites (Figure 3a), conforming to previous findings (Busch et al., 2006; Herrmann et al., 1999; Martinovic et al., 2007; Tallon-Baudry et al., 1997). Evoked GBA between 50 and

150 ms in the 30-40 Hz range was not significantly modulated across conditions (see Table 3).

Spectral amplitude induced by picture presentations showed a clear peak in a time window from approx. 180 to 350 ms after stimulus onset in a frequency range between 35 and 90 Hz (Figure 2b).

---

insert Figure 3 about here

For induced GBA individual frequencies with greatest amplitude ranged between 30 and 90 Hz (54.44 ± 2.87 Hz). Average frequencies of the highest amplitude wavelet were 52.08 ± 3.22 Hz for 0°, 55.97 ± 4.06 Hz for ±60°, and 51.94 ± 3.21 Hz for ±120° condition. There were no significant differences between frequencies at which highest induced GBA was observed for each condition ($F(2,17) = 0.53$, n.s.) thus excluding the possibility that results were biased by systematic frequency differences. In our peak-picking approach all three conditions were subsequently collapsed and the individual maximal wavelets (i.e., the centre of the ±5 Hz frequency bands) were selected from TF plots of a mean across conditions (as described in the methods section).

Topographical distribution of induced gamma amplitude, computed for ± 5 Hz frequency bands centred on the individual maximal wavelet in the time window of maximal amplitude, collapsed across all three conditions is shown in Figure 3b.

Conforming to previous findings (Gruber et al., 2002; Gruber et al., 2004) induced GBA had a relatively broad scalp distribution, with a pronounced posterior activity, centred upon parietal sites and extending into the parieto-occipital sites.

Grand-mean induced GBA, defined as the amplitude in the ±5 Hz frequency band centred on the individual maximal wavelet in the time window 180 to 350 ms at the selected parietal sites after baseline subtraction, was significant when tested against zero revealing induced gamma-band peaks were clearly present (0°, $t(17) = 6.67$; ±60°, $t(17) = 4.88$; ±120°, $t(17) = 6.60$; for all conditions, $p < 0.001$).

As expected statistical comparisons of induced gamma-band amplitude showed no significant differences between conditions.

Repeated measures ANOVA with the factor CONDITION (0°, ±60° and ±120°) showed a significant effect for peak latencies of induced GBA. As enumerated in Table 3 and also in Figure 4 (means and latency distributions) and Figure 5 (time courses) peak latency was delayed as a function of orientation. Post-hoc t-tests revealed this was mostly due to a significant delay between 0° and ±120° ($t(17) = -2.4$, $p < 0.05$) and a strong delay trend between 0° and ±60° ($t(17) = -2.0$, $p = 0.06$). There was no difference between ±60° and ±120° conditions ($t(17) = -0.86$, n.s.).

---

insert Figure 4 about here

Figure 5a shows the time-course of the grand-mean induced GBA in the 52.5-57.5 Hz range (i.e., around the 55 Hz wavelet which was identified as the central frequency across all participants) whereas Figure 5b shows the time-course of activity in the ±5 Hz band around the individual maximal wavelet for a representative participant. While averaging of data in Figure 5a has somewhat masked the observed latency delays, blending them into a more

general shift in the distribution of amplitude, the time-course for the representative participant in Figure 5b demonstrates clear delay effects.

Observed latency delays in the induced GBA peak did not correlate with RT delays when Spearman's coefficient correlations were calculated across participants (±60° delays, rs = -0.10, n.s.; ±120° delays, rs = -0.31, n.s.).

---

insert Figure 5 about here

Statistical parametric maps (SPMs; axial, sagittal and coronal slices) of the induced GBA peak for each condition are shown in Figure 6a while SPMs of differential activity between disoriented and upright conditions are depicted in Figure 6b.

---

insert Figure 6 about here

Induced GBA generators were widespread across source space with activity distributed across bilateral prefrontal, temporal and posterior locations. Medial prefrontal activity was particularly pronounced for disoriented objects, spreading into the inferior frontal gyrus. Table 4 provides Montreal Neuroscience Institute (MNI) coordinates of the significantly activated sources and also gives their brief anatomical descriptions.

---

insert Table 4 about here

---

3. Discussion

The study had three major aims: (1) replicate the findings of Martinovic et al. (2007) with an improved plane-rotation paradigm; (2) assess the validity of the covert naming task in obtaining recognition-related RT delays; and (3) complement the findings on induced GBA peak latency delays through source localisation. Just as in the previous study a plane-rotation paradigm was used in order to elicit view-dependent processing of disoriented objects. A covert naming task (gender decision) was used in order to measure the delays in recognition that occur for disoriented objects. First, the task was successfully validated in a control experiment. The EEG experiment replicated the induced GBA peak latency delays for disoriented objects. Looking at the sources of neural activity allowed us to ascertain that adaptive changes in underlying neuronal generators lay behind the modulated distribution of the induced GBA. Relative contribution of posterior, temporal and prefrontal sources differed between upright and disoriented objects: prefrontal activity became more prominent with increased disorientation. These findings throw further light on the assumed role of induced GBA as EEG markers of cortical object representation.

In our previous study, an EEG-compatible paradigm aimed at accessing entry-level identification, the level objects are recognised in everyday life, was tested. The study demonstrated that covert naming tasks can be successfully used for that purpose. As a further improvement, the present experiment controlled for basic differences between objects in naming times by counterbalancing the assignment of stimuli to conditions across the sample.

Such a procedure is preferable to fixing the assignment of stimuli to conditions as in Martinovic et al. (2007). Effects of plane-rotation on the recognisability of each image are nonlinear. Thus, one item might be easier to recognise at 300° than at 120° of rotation while for another the opposite might be the case. Because of these item-specific effects of orientation controlling for naming speeds at 0° is not fully adequate – even if the two objects take the same amount of time to name when upright, differences in naming speed between them can reappear once they become disoriented. For this reason stimulus counterbalancing across the sample is often used in studies on view-dependent object identification (see, for example Lawson and Jolicoeur, 2003; Murray, 1995c).

The second major change from our previous study concerned the task that was used to elicit the so-called covert naming. Instead of a phonological judgment on the identity of the first letter of the name a grammatical gender decision was used. This syntactic task is well suited to the German language, which contains three genders: masculine, feminine and neutral. Grammatical gender is a lexical property of words and it is often used in implicit naming paradigms that aim to examine the time course of syntactic processing (see Schmitt et al., 2001). It is mostly arbitrary but can also be influenced by semantic or phonological factors (Schiller et al., 2003) due to certain words having biological gender and other words being gender-marked by certain phonological regularities. While interactions between semantic and syntactic factors occur at later processing stages, ERPs have shown that early streams are autonomous (Gunter et al., 2000).

To further verify the degree of similarity between overt naming and the newly implemented covert task, a control experiment was performed in which they were directly contrasted. Accuracy rates between overt and covert tasks were comparable whereas gender decision times (i.e. covert naming) were on average 200-300 ms longer, reflecting the additional requirement of making a syntactic judgement on the object's name. The effects of

disorientation were smaller than in previous studies (e.g., Murray, 1995c) but consistent with Martinovic et al. (2007). The results imply this cannot be due to the nature of the covert task as reduced delays were even more pronounced for overt naming. In fact, in overt naming the delay between ±60° and ±120° was particularly reduced, as were the accuracies, which fell to about 70% while in typical overt naming they usually stay near 100%. However, linear increases with disorientation were identified for both overt and covert tasks, which fits with classical findings on the linear type of disorientation delays in plane-rotation paradigms (e.g., Jolicoeur, 1985; McMullen and Jolicoeur, 1990; Murray, 1995a). Smaller delays than those in previous studies, as well as lower accuracy rates, should thus be attributed to large variability of the stimulus set. It included many objects with compound names such as seahorse, lawnmower and wheelchair as well as infrequent names such as easel and wheelbarrow; these items are generally not used in overt naming behavioural studies which can rely on smaller stimulus sets than EEG.

However, in spite of these discrepancies between the two tasks, a highly significant correlation of RTs was found in an across item analysis. The fact that this correlation resurfaces across items but not across participants, who saw different images in different conditions, confirms the main assumption that overt and covert tasks access common recognition processes. The tasks are likely to differ in their relative reliance on linguistic processes and response production mechanisms, which would explain that the correlation is small in spite of its high significance. Based on this, we conclude that the novel EEG-compatible covert naming paradigm provides a very useful contribution to future neurophysiological studies on object recognition. It will allow future EEG studies to elicit the entry-level of object identification at which view-dependent processing can occur.

The main hypothesis of the EEG experiment was also confirmed: peak latency of induced GBA was again related to recognition delays for disoriented objects, elicited by the plane-

rotation paradigm. The behavioural effects in our experiment were also more robust then those in Martinovic et al. (2007). Significant RT delays were obtained between all three conditions (upright, ±60° and ±120°). The peak latency of induced GBA at broad parieto-occipital sites was significantly delayed for ±120° rotated objects when compared to upright objects, while a pronounced trend for delays was observed for ±60° rotated objects. This modulation was again present selectively for induced GBA peak latency. No such effect was observed in the ERPs or induced gamma amplitude and evoked gamma-band activity also remained unmodulated.

Localisation of generators of neuronal activity in source space indicated that a widespread distributed set of bilateral prefrontal, temporal and posterior regions stood behind the induced GBA. A previous study by Gruber et al. (2006) examined neuronal sources of object categorisation at the superordinate level. At the superordinate level items are classified as an animal or a non-animal. At entry-level, which was elicited in this study, items are classified as a tiger, bird, bear or light bulb, bottle or table. In their study, Gruber et al. (2006) found that induced GBA was generated in left inferior temporal and lateral occipitotemporal (fusiform) gyri, bilateral superior and middle parietal and occipital areas and in right middle frontal and precentral gyri. The observed generators for upright objects in the present study largely overlapped with these areas, with the notable exception that bilateral middle frontal activity was present for entry-level recognition. In fact these prefrontal areas were shown to play an important role, enlarging their contribution to the induced GBA with increases in disorientation. Meanwhile, temporal and posterior sources decreased their high frequency oscillatory activity relative to prefrontal generators for disoriented items. Such adaptive changes in coding fit very well with existing findings and proposed models of object identification. Involvement of medial and inferior parts of prefrontal lobes, which play a significant role in memory encoding and retrieval (Cabeza and Nyberg, 2000; Nyberg et al.,

2003) and semantic discrimination (Otten and Rugg, 2001). Their involvement supports previous arguments that induced GBA is crucially related to late representational processes that subserve visual memory (Gruber et al., 2004; Gruber and Müller, 2005; Martinovic et al., 2007). Involved areas also lie in the vicinity of orbito-frontal cortex and our spatial resolution of approx. 11 mm combined with a localization error of approx. 14 mm (Trujillo-Barreto et al., 2004) cannot discount an overlap of activity. This is in general accordance with the model proposed by Bar (2003) which supposes that feedback into representational areas guides the selection between candidate templates that have resulted from bottom-up processing in posterior and temporal areas. Top-down feedback into the visual cortex has already been implicated to play a role in successful encoding (Takashima et al., 2006) and recognition (Bar et al., 2006) of visually presented objects. According to our findings it is therefore highly likely that flexible changes in coding occurred between the generators of induced GBA. Sources have been led to shift from more bottom-up representational processing to top-down driven identification by increasing disorientation and it is possible to conclude that this shift is likely to complement the observed latency delay in induced GBA.

This study, like Martinovic et al. (2007), failed to obtain correlations between RT delays and induced GBA delays. It has been observed that performance correlated changes in object representation occur in prefrontal cortex neurons but not in inferior temporal neurons (Rainer and Miller, 2000). Correlations between behavioural and neurophysiological measures of repetition priming have not been found in a study that measured the activity of IT neurons in monkey cortex (McMahon and Olson, 2007). These authors discuss that changes in the representational activity of IT neurons could result in enhanced post-synaptic efficacy and stronger firing in areas of frontal cortex that receive projections from IT cortex (also supported by van Turennout et al., 2000). Indeed source localisation in this study indicated that the crucial adaptive change occurred in the enhancement of activity within prefrontal

areas. As widespread sources are involved in the generation of induced GBA, it is possible that the lack of correlation is due to the overlap of prefrontal, posterior and temporal neuronal activity in the measured response. This is not purely a signal-to-noise issue. A possible solution would lie in intracortical measuring of induced GBA's latency as it moves through cortical areas along the ventral pathway, as in Lachaux et al.'s (2004) study. Due to their high signal-to-noise ratio and area-specificity intracortical recordings have already succeeded in revealing correlations between induced GBA latency and representational activity (e.g., see Womelsdorf et al., 2006).

In summary, this study confirmed the relation first observed in Martinovic et al. (2007) wherein recognition time delays were accompanied by induced gamma-band latency delays. A shift in the relative activity of induced GBA generators between upright and disoriented objects accompanied the latency delay: with increased disorientation prefrontal activity became more prominent. This is likely to indicate a shift from bottom-up to top-down processing, occurring because of additional template-matching requirements in successful recognition and encoding of disoriented objects. This finding further strengthens the proposal that induced GBA reflects the later stream of representational processing connected to visual memory. It is now possible to assert that adaptive changes in dynamic coding of object identity occur during recognition of disoriented objects. In this study induced GBA was again shown to be a marker that is selectively sensitive to these changes. This provides further evidence that induced high frequency oscillatory activity in the human brain forms a robust neural signature of representational activity in high-level vision.

4. Experimental Procedure

4.1. Control Experiment

4.1.1. Participants

12 healthy university students (7 female; aged 19 - 27 years, mean age = 23 years) received class credit or a small honorarium for participating in the study. Participants reported normal or corrected-to-normal vision and all were native speakers of German. Individual written informed consent was obtained and the study conformed to the Code of Ethics of the World Medical Association.

4.1.2. Materials and procedure

The stimulus set of 204 pictures and the practice set of 36 pictures were a result of a limited pilot study conducted with a preliminary set of images in order to evaluate the suitability of the selected stimuli and reassess their dominant names, focusing on their grammatical gender. Images were selected from existing stimulus sets (International Picture Naming Project with German norms containing 525 pictures - Bates et al., 2003; 400 pictures from a French-language naming study - Alario and Ferrand, 1999; and 152 images used in object recognition studies - Hamm, 1997).

All of the objects represented in the stimulus set had a predominant environmental orientation which was labelled as 0° (i.e., upright). Disoriented pictures were created by rotating the upright picture by 60°, 120°, 240° and 300° in the frontal picture plane. The 180° rotation was not used as it produces RTs that are somewhat shorter than expected and very variable (Lawson and Jolicoeur, 2003) due to different possible ways in which image normalisation can be achieved; transformation as in other conditions or flipping-over in the

image-plane. Stimulus presentation occurred in a random order and was different for each participant.

Presentation of stimulus images was counterbalanced across the sample so that every item appeared in each of the three orientations (upright, ±60° and ±120°; with disoriented images being equally distributed into 60°/300° and 120°/240° respectively) an equal number of times. Therefore stimulus presentation lists were generated in a balanced fashion for six participants at a time thus ensuring each image was assigned for presentation in an upright ±60° (split evenly between 60° and 300°) and ±120° (split evenly between 120° and 240°) position for two of the six participants. In addition stimulus lists were generated in a way that ensured each object would be assigned to both tasks with equal frequency. This was done by inverting the assignment-to-task for the six counterbalanced stimulus lists thereby obtaining a set of lists for all of the planned 12 participants. Across the whole sample each picture was presented in each condition (upright, ±60° and ±120°) for a total of two times and if one participant named it covertly a matched participant would name it overtly (and vice versa). This ensured that while all objects were represented in all conditions across the sample every participant saw just one version of the same object. As explained in the discussion, this is a common procedure (e.g., Murray, 1998) used to control for item-specific effects.

Task order was counterbalanced between participants so that one half started with overt naming and the other half with gender decision. Overt naming was carried out in a typical way with participants instructed to say the first name that came to mind upon seeing the image of the object. Speech-onset latencies were measured from the onset of the target picture with a voice-key connected to a computer. The experimenter monitored whether participants used the expected target names and coded erroneous responses.

The covert naming task required participants to press one of three buttons, using index, middle and ring fingers of one hand, depending on the grammatical gender of object's

name, i.e. masculine, feminine or neutral. They were instructed to perform this syntactic judgment based on the definitive determiner ('der', 'die' or 'das')[3] of the first correct name that came to mind after seeing the picture. They indicated their response by pressing the buttons corresponding to these determiners ('1', '2' or '3'). Among the 204 objects presented there were 68 for each of the three genders. Key-to-task allocation was not counterbalanced across participants due to the over-learnt nature of gender label order, i.e., 'der' being first, followed by 'die' and 'das'. Half way through the experiment participants were asked to change the responding hand.

Before each of the two tasks, participants performed a practice block of 18 trials that contained a subset of stimuli not used in the experiment itself. This was followed by two blocks of 51 trials for each task, each lasting approximately three minutes. Each trial consisted of a 600 ms baseline period, during which a black fixation cross (0.3° x 0.3°) was presented. This was followed by a stimulus picture that was displayed for 650 ms; this was then replaced by the fixation cross that remained on screen for a period of 1650 ms.

Stimuli were presented centrally on a 19-inch flat screen monitor with a 120 Hz refresh rate that was positioned 1m in front of the participant. Images of objects, subtending a visual angle of approx. 5 x 5°, were all shown in black on a white background. Timing of the presentation of the stimuli and data collection were controlled by NESU (Nijmegen Experimental Setup).

4.1.3. Data analysis

To match the parameters of the previous study (Martinovic et al., 2007) only correct trials with RTs between 400 and 2300 ms were taken into analysis.

[3] These are German definite articles that precede a noun and mark its gender (masculine, feminine or neutral) in nominative case.

Accuracy rates were analysed across participants while RTs on correctly answered trials were analysed both across participants and across items. For the overt naming task, observations were coded as erroneous and discarded from the reaction time analysis whenever a picture had not been named with the expected name, the voice-key was triggered by a non speech sound, or the utterance was dysfluent.

In the across participant analysis median RTs were computed for each participant; using medians is consistent with previous studies that employed plane-rotation paradigms (e.g., Jolicoeur et al., 1998) due to the skewness of RT distributions. We then computed means across participants to obtain a measure of central tendency known as a mean of median RT (for a similar procedure, see Murray, 1995b). In the across item analysis overall medians as well as means and their standard errors were computed.

Across participants, 2x3 repeated measures ANOVA with the factors of naming type (overt or covert) and degree of rotation (upright, ±60° and ±120°) was performed on accuracy rates and RTs. Repeated measure ANOVAs were subsequently performed within every naming task separately to ascertain the exact effects of disorientation in each. Across items, one-way ANOVA with the factor of condition (upright, ±60° and ±120°) was performed within every naming task.

Correlations of accuracies and RTs within every naming task were performed in order to check for possible speed-accuracy trade-offs. Correlations of RTs between the two tasks were performed both across participants and across items in order to establish the relation between the two tasks.

Greenhouse-Geisser correction for multiple comparisons was used when necessary. Post-hoc analyses were carried out using paired t-tests.

4.2. EEG Experiment

4.2.1. Participants

24 healthy, right-handed university students received class credit or a small honorarium for participating in the study. Six participants had to be removed; three because of technical problems during the recording, one due to excessive EEG artifacts and two due to the absence of GBA. The final sample therefore consisted of 18 participants (10 female; aged 19 - 34 years, mean age = 24 years) who reported normal or corrected-to-normal vision and were all native speakers of German. None of them had participated in picture recognition studies in the previous six months. Individual written informed consent was obtained and the study conformed to the Code of Ethics of the World Medical Association.

4.2.2. Materials and procedure

The stimulus set of 204 pictures and the practice set of 36 pictures from the control experiment were used. As described stimuli were counterbalanced across the sample so that every image appeared in each of the three orientations (upright, ±60° and ±120° - with disoriented images being equally distributed into 60°/300° and 120°/240°) an equal number of times across the sample. For example, one participant would see a picture of a certain object in its upright position, another one in the 60° disoriented position, a third one in 120°, and so forth. In addition, to avoid previously reported repetition suppression effects in the induced GBA (Fiebach et al., 2005; Gruber et al., 2002; Gruber et al., 2004) a different object was depicted in every experimental trial. To summarise, only a single image of a particular stimulus object was shown to each of the participants during the experiment. However, across all the participants, each object was shown equally often in each of the three conditions

(upright, ±60° and ±120°). Stimulus presentation occurred in a random order and was different for each participant.

Participants performed the same grammatical gender judgment as in the control experiment. They were instructed to minimise eye movements and blinking during the display of a stimulus or the fixation cross. Feedback was not provided after each individual trial but at the end of each block. Two measures, average percent correct and average RT, were computed on the basis of all the trials in that block and were shown to the participants. If their performance fell below the levels expected based on the control experiment they were encouraged to try and respond faster or more accurately.

Participants first performed a practice block of 36 trials that contained a subset of stimuli not used in the experimental trials. The experiment consisted of four 51 trial blocks each lasting approximately three and a half minutes. Each trial consisted of a variable 500-700 ms baseline period during which a black fixation cross (0.3° x 0.3°) was presented. Following this a stimulus picture was displayed for 650 ms which was subsequently replaced by the fixation cross that remained on the screen for a period of 1650 ms.

Stimuli were presented centrally on a 19-inch computer screen with a 70 Hz refresh rate that was positioned 1.5 meters in front of the participant in a dimly lit soundproof testing chamber. Images of objects, subtending a visual angle of approx. 4.5 x 4.5°, were all shown in black on a white background. Stimulus onset was synchronised to the vertical retrace of the monitor.

4.2.3. EEG recording

EEG was recorded continuously from 128 locations using active Ag-AgCl electrodes (BioSemi Active-Two amplifier system; Biosemi, Amsterdam, The Netherlands) placed in an elastic cap. In this system the typically-used ‘ground’ electrodes in other EEG amplifiers are

replaced through the use of two additional active electrodes, positioned in close proximity to the electrode Cz of the international 10-20 system (Jasper, 1958): Common Mode Sense (CMS) acts as a recording reference and Driven Right Leg (DRL) serves as ground (Metting Van Rijn et al., 1990; Metting Van Rijn et al., 1991). Horizontal and vertical electrooculograms were recorded in order to exclude trials with blinks and significant eye movements.

EEG signal was sampled at a rate of 512 Hz and was segmented into epochs starting 500 ms prior and lasting 1500 ms following picture onset. EEG data processing was performed using the EEGlab toolbox (Delorme and Makeig, 2004) combined with in-house procedures running under the Matlab (The Mathworks, Inc) environment. Artifact correction was performed by means of 'statistical correction of artefacts in dense array studies' (SCADS; Junghöfer et al., 2000). It is widely accepted in the field and has been applied and described in several publications (Gruber et al., 1999; Martinovic et al., 2007; Müller and Keil, 2004).

All incorrectly answered trials were excluded prior to data analysis. The average rejection rate was 25.1 %, resulting in approx. 43 remaining trials per condition. Further analyses were performed using the average reference.

4.2.4. Behavioural data analysis

RTs between 400 and 2300 ms, the maximum time allowed for responses, for trials with correct responses were taken into further analysis.

As in the control experiment median RTs for correct items were computed for each participant. Means across participants were then computed to obtain a measure of central tendency known as a mean of median RT. Differences in mean of median RTs for each participant were calculated by subtracting the average upright naming time from RT for 60°

and 120°. Therefore for each participant two delay scores were computed: RT delay for 60° and for 120° conditions.

Differences in naming speed between the three conditions were analysed with a repeated measures ANOVA comprising the factor of CONDITION (upright, ±60° and ±120°). Post-hoc tests were performed using paired t-tests.

4.2.5. Event related potentials (ERPs) analysis

A 25 Hz low-pass filter was applied to the data before all ERP analyses. Identical to our previous study, three ERP components were assessed; N1, P300 and parietal negativity. Table 2 (see Results) lists the analysis windows and electrode sites taken into the regional mean for each component (also shown in Figure 7). Mean amplitude within the

---

insert Figure 7 about here

---

respective time window was calculated for each component and the mean amplitude during the period 100 ms prior to stimulus onset (baseline) was subtracted. Each component was subject to repeated measures ANOVA comprising the factor of CONDITION (upright, ±60° and ±120°). Post-hoc tests were performed using paired t-tests.

4.2.6. Analysis of Evoked and Induced Spectral Changes

Induced oscillatory activity was analysed according to the standard procedure employed in many previous studies (e.g., Gruber et al., 2004; Gruber and Müller, 2005; Martinovic et al., 2007). In brief, spectral changes in oscillatory activity were analysed by

means of Morlet wavelet analysis (Bertrand and Pantev, 1994), which offers a good compromise between time and frequency resolution (Tallon-Baudry and Bertrand, 1999). This method provides a time-varying magnitude of the signal in each frequency band leading to a time-by-frequency (TF) representation of the signal and, together with suggested parameter definitions that allow for a good time and frequency resolution in the gamma frequency range, is detailed in previous studies (e.g., Gruber and Müller, 2005). In order to achieve good time and frequency resolution in the gamma frequency range, the wavelet family in this study was defined by a constant $m= f_0/\sigma_f = 7$, with f_0 ranging from 2.5 to 100 Hz in 0.5 Hz steps. This data was subsequently reduced to form 2.5 Hz-wide wavelets. Time-varying energy in a given frequency band was calculated for each epoch by taking the absolute value of the convolution of the signal with the wavelet.

Preliminary electrode sites used for time-by-frequency plots were selected on the basis of previous findings of maximal local gamma power elicited by object identification paradigms; parietal for induced GBA (Gruber et al., 2004; Gruber and Müller, 2005; Martinovic et al., 2007) and occipital for evoked GBA (Busch et al., 2006; Herrmann et al., 1999; Martinovic et al., 2007; Tallon-Baudry et al., 1997). These sites were further readjusted in order to envelop the area of maximal amplitude for data collapsed across conditions in case the observed grand mean topography happened to differ from previous findings. Maps of oscillatory responses in the ±5 Hz frequency band centred upon the maximal activity wavelet for each participant during the time window of maximal activity were calculated by means of spherical spline interpolations (Perrin et al., 1988).

In order to identify the time window and frequency range of the induced GBA peaks mean baseline-corrected spectral amplitude (baseline: 100 ms prior to stimulus onset) was collapsed together for all conditions and represented in TF-plots in the 30-90 Hz range. The length of the time window of maximal gamma-band amplitude was defined based on the

observed grand-mean GBA, a common approach in previous studies (e.g., Busch et al., 2004; Gruber and Müller, 2005).

Regional means of interest were determined on the basis of grand mean topographies. Due to inter-individual differences in the induced gamma peak in the frequency domain a specific wavelet for each participant was chosen based on the frequency of his/her maximal amplitude in an average across all three conditions. Centred upon this wavelet a frequency band of ±5 Hz was subsequently formed for the purpose of statistical analyses.

Frequencies of individual maximal wavelets were also identified for each separate condition on TF-plots of mean baseline-corrected spectral amplitudes. This was done only in order to verify that the selected maximal wavelets (i.e., the centre of the ±5 Hz frequency bands) represented all three conditions equally. Consistent with our previous study, no differences were expected between the conditions in the frequencies of maximal amplitude.

The peak latency of GBA was defined as the latency of maximal amplitude within the ± 5 Hz frequency band centred upon the individual maximal wavelet (see Martinovic et al., 2007; Posada et al., 2003; Tallon-Baudry et al., 1996). The basis of such a definition relies on computation methods that define the time-resolution of the Morlet wavelet analysis. When wavelet convolutions are computed the convolution peaks at the same latency as the respective frequency component in the raw data, smearing the peak width due to responses being quite jittered between trials; sometimes up to 80ms or more. In other words, a gamma band peak will maintain its latency throughout the range of frequencies involved but its overall amplitude will end up being somewhat smeared across the sample. Therefore our peak-picking approach maintains the highest level of objectivity when comparing latency across different conditions.

For induced GBA, differences between conditions in the central frequencies of gamma-band activity at the regional mean, the amplitude of the gamma peak after baseline

subtraction and the latency of its maximal local amplitude were evaluated by means of repeated measures ANOVA with the factor CONDITION (upright, ±60° and ±120° rotation).

To enable us to relate the delays in induced GBA with delays in naming RTs, peak latency delays were computed to correspond with RT delays (described in behavioural methods). The peak latency for upright was subtracted from peak latencies for both ±60° and ±120° thus obtaining measures of induced GBA peak latency delays. In order to see if the relations between these two measures were indirect or direct, induced GBRs latency delays and RT delays were correlated using Spearman's coefficient.

Evoked oscillatory activity is by definition time- and phase-locked to stimulus onset and was analysed through a transformation of the unfiltered ERP into the frequency domain. Evoked GBA has low inter-individual variability and in object categorisation studies that use line-drawings it is usually observed at frequencies between 30 and 40 Hz, with maximal activity usually occurring in a narrow time interval around 50-150 ms post stimulus-onset (e.g., Gruber et al., 2004; Gruber and Müller, 2005; Martinovic et al., 2007). Therefore a ±5 Hz range was taken around a central wavelet of 35 Hz within a time window of 50-150 ms. For evoked GBA, differences between conditions at the regional mean sites (see Figure 3, Results), the amplitude after baseline subtraction and the latency of its maximal local amplitude were analysed by means of a repeated measurement ANOVA with the factor CONDITION (upright, ±60° and ±120°).

Means and standard errors of the mean are reported throughout the results section. All post-hoc tests were conducted using paired t-tests.

4.2.7. Source modelling (VARETA)

To reconstruct the estimated sources of the observed effects in the time and frequency domain an adaptation of VARETA (**Va**riable **Re**solution **E**lectromagnetic **T**omogr**a**phy) was used. A detailed description of this approach can be found elsewhere (Bosch-Bayard et al.,

2004; Gruber et al., 2006; Trujillo-Barreto et al., 2004). In brief, VARETA estimates the spatially smoothest generator-estimates compatible with the observed scalp topographies and places anatomical constraints upon the allowable solutions. The generators of the EEG data inside the brain are mapped by using a three dimensional (3D) grid of points (or voxels) that represent possible sources of the signal and for which the probability for grey matter is different from zero (based on the average probabilistic brain atlas produced by the Montreal Neurological Institute; Evans et al., 1993).

To uncover the sources of induced GBA peaks single trials were first transformed into the frequency domain. Subsequently, single trial estimates of the primary current densities in source space (i.e. at the predefined 3D grid locations) are computed during the time window of maximal activity for the ±5 Hz bands around the individually selected gamma peak wavelets (see gamma-band analysis methods, above). Single trial activity was previously scaled by a global scale factor (GSF; Hernandez et al., 1995) which takes into account complex wavelet coefficient for the full range of gamma-band frequencies during the baseline period (for a full formula and explanation, see Gruber et al., 2006.) The spectrum of the inverse solution for each trial and in each voxel was then calculated and averaged across the time window of interest.

Sources of activation were analysed for each individual condition. In order to localise the differences in activation between the conditions the primary current densities related to condition 'upright' were subtracted from condition '±60°' and condition '±120°'. Statistical comparisons were then carried out by means of a voxel by voxel Hottelling T2 test against zero.

Activation threshold correction to account for spatial dependencies between voxels was calculated by means of Random Field Theory (Worsley et al., 1996). The statistical

parametric maps (SPMs) were then projected onto coronal, axial and sagittal planes and were thresholded at a significance level of $p<0.01$.

Acknowledgements

We would like to thank Renate Zahn, Martin Cziuppa and Sophie Trauer for help with data acquisition and Søren Andersen for technical assistance. We would also like to thank Anthony Martyr for proofreading the manuscript. The Deutsche Forschungsgemeinschaft supported this research. J.M. was supported by the Deutscher Akademischer Austausch Dienst (DAAD).

References

Alario, F. X., Ferrand, L., 1999. A set of 400 pictures standardized for French: Norms for name agreement, image agreement, familiarity, visual complexity, image variability, and age of acquisition. Behav. Res. Methods. 31**,** 531-552.

Bar, M., 2003. A cortical mechanism for triggering top-down facilitation in visual object recognition. J. Cogn. Neurosci. 15**,** 600–609.

Bar, M., Kassam, K. S., Ghuman, A. S., Boshyan, J., Schmid, A. M., Dale, A. M., Hämäläinen, M. S., Marinkovic, K., Schacter, D. L., Rosen, B. R., Halgren, E., 2006. Top-down facilitation of visual recognition. Proc. Natl. Acad. Sci. U. S. A. 103**,** 449-454.

Bates, E., D'Amico, S., Jacobsen, T., Szekely, A., Andonova, E., Devescovi, A., Herron, D., Lu, C. C., Pechmann, T., Pleh, C., Wicha, N., Federmeier, K., Gerdjikova, I., Gutierrez, G., Hung, D., Hsu, J., Iyer, G., Kohnert, K., Mehotcheva, T., Orozco-Figueroa, A., Tzeng, A., Tzeng, O., 2003. Timed picture naming in seven languages. Psychonomic Bulletin & Review. 10**,** 344-380.

Bertrand, O., Pantev, C., Stimulus frequency dependence of the transient oscillatory auditory evoked response (40 Hz) studied by electric and magnetic recordings in human. In: C. Pantev, T. Elbert, B. Lütkenhöner, Eds., Oscillatory Event-Related Brain Dynamics. NATO ASI Series, vol. Plenum Press, New York, USA, 1994, pp. 231-242.

Bosch-Bayard, J., Valdés-Sosa, P., Virués-Alba, E., Aubert-Vázquez, E., John, R., Harmony, T., Riera-Díaz, J., Trujillo-Barreto, N., 2004. 3D statistical parametric mapping of variable resolution electromagnetic tomography (VARETA). Clin Electroencephalogr. 32**,** 47-66.

Busch, N. A., Debener, S., Kranczioch, C., Engel, A. K., Herrmann, C. S., 2004. Size matters: effects of stimulus size, duration and eccentricity on the visual gamma-band response. Clin. Neurophysiol. 115**,** 1810-1820.

Busch, N. A., Herrmann, C. S., Müller, M. M., Lenz, D., Gruber, T., 2006. A cross-lab study of event-related gamma activity in a standard object-recognition paradigm. Neuroimage. 33**,** 1169-1177.

Cabeza, R., Nyberg, L., 2000. Imaging cognition II: An empirical review of 275 PET and fMRI studies. J. Cogn. Neurosci. 12**,** 1-47.

Delorme, A., Makeig, S., 2004. EEGLAB: an open source toolbox for analysis of single-trial EEG dynamics including independent component analysis. . J. Neurosci. Methods. 134**,** 9-21.

Dux, P. E., Harris, I. M., 2007. Viewpoint costs occur during consolidation: Evidence from the attentional blink. Cognition. 104**,** 47-58.

Evans, A. C., Collins, D. L., Mills, S. R., Brown, E. D., Kelly, R. L., Peters, T. M., 1993. 3D statistical neuroanatomical models from 305 MRI volumes, vol. 95. M.T.P Press, London.

Fiebach, C. J., Gruber, T., Supp, G. G., 2005. Neuronal mechanisms of repetition priming in occipitotemporal cortex: spatiotemporal evidence from functional magnetic resonance imaging and electroencephalography. J. Neurosci. 25**,** 3414-3422.

Gruber, T., Keil, A., Müller, M. M., 2002. Modulation of human induced gamma band response in a perceptual learning task. J. Cogn. Neurosci. 14.

Gruber, T., Malinowski, P., Müller, M. M., 2004. Modulation of oscillatory brain activity and evoked potentials in a repetition priming task in the human EEG. Eur. J. Neurosci. 19**,** 1073-1082.

Gruber, T., Müller, M. M., 2005. Oscillatory brain activity dissociates between associative stimulus content in a repetition priming task in the human EEG. Cereb. Cortex. 15**,** 109—116.

Gruber, T., Müller, M. M., Keil, A., Elbert, T., 1999. Selective visual-spatial attention alters induced gamma band responses in the human EEG. Clin. Neurophysiol. 110**,** 2074-2085.

Gruber, T., Trujillo-Barreto, J. N., Giabbiconi, C. M., Valdes-Sosa, P. A., Müller, M. M., 2006. Brain electrical tomography (BET) analysis of induced gamma band responses during a simple object recognition task. Neuroimage. 29**,** 888-900.

Gunter, T. C., Friederici, A. D., Schriefers, H., 2000. Syntactic gender and semantic expectancy: ERPs reveal early autonomy and late interaction. J. Cogn. Neurosci. 12**,** 556-568.

Hamm, J. P., Object orientation and levels of identity. Vol. PhD Thesis. Dalhousie University, Halifax, 1997.

Harris, I. M., Dux, P. E., 2005. Tuning objects on their heads: The influence of the stored axis on object individuation. Percept. Psychophys. 67**,** 1010-1015.

Hernandez, J. L., Valdes, P., Biscay, R., Virues, T., Szava, S., Bosch, J., Riquenes, A., Clark, I., 1995. A global scale factor in brain topography. Int. J. Neurosci. 76**,** 267-278.

Herrmann, C. S., Mecklinger, A., Pfeifer, E., 1999. Gamma responses and ERPs in a visual classification task. Clin. Neurophysiol. 110**,** 636-642.

Jasper, H., 1958. The ten-twenty electrode system of the International Federation. Electroencephalogr. Clin. Neurophysiol. 10**,** 371-375.

Jolicoeur, P., 1985. The time to name disoriented natural objects. Mem. Cognit. 13**,** 289-303.

Jolicoeur, P., Corballis, M. C., Lawson, R., 1998. The influence of perceived rotary motion on the recognition of rotated objects. Psychonomic Bulletin & Review. 5**,** 140-146.

Junghöfer, M., Elbert, T., Tucker, D. M., Braun, C., 2000. Statistical control of artifacts in dense array EEG/MEG studies. Psychophysiology. 37**,** 523-532.

Kaiser, J., Buhler, M., Lutzenberger, W., 2004. Magnetoencephalographic gamma-band responses to illusory triangles in humans. Neuroimage. 23**,** 551-560.

Karakas, S., Basar, E., 1998. Early gamma response is sensory in origin: a conclusion based on cross-comparison of results from multiple experimental paradigms. Int. J. Psychophysiol. 31**,** 13-31.
Lachaux, J.-P., George, N., Tallon-Baudry, C., Martinerie, J., Hugueville, L., Minotti, L., Kahane, P., Renault, B., 2005. The many faces of the gamma band response to complex visual stimuli. Neuroimage. 25**,** 491-501.
Lawson, R., Jolicoeur, P., 2003. Recognition thresholds for plane-rotated pictures of familiar objects. Acta Psychol. (Amst.). 112**,** 17–41.
Martinovic, J., Gruber, T., Müller, M. M., 2007. Induced gamma-band responses predict recognition delays during object identification. J. Cogn. Neurosci. 19**,** pp.1-14.
McMahon, D. B. T., Olson, C. R., 2007. Repetition supression in monkey inferotemporal cortex: relation to behavioral priming. J. Neurophysiol. 97**,** 3532-3543.
McMullen, P. A., Jolicoeur, P., 1990. The spatial frame of reference in object naming and discrimination of left-right reflections. Mem. Cognit. 18**,** 99-115.
Metting Van Rijn, A. C., Peper, A., Grimbergen, C. A., 1990. High quality recording of bioelectric events: I: interference reduction, theory and practice. Med. Biol. Eng. Comput. 28**,** 389-397.
Metting Van Rijn, A. C., Peper, A., Grimbergen, C. A., 1991. High quality recording of bioelectric events. II: a low noise low-power multichannel amplifier design. Med. Biol. Eng. Comput. 29.
Müller, M. M., Keil, A., 2004. Neuronal synchronization and selective color processing in the human brain. J. Cogn. Neurosci. 16**,** 503-522.
Murray, J. E., 1995a. Imagining and naming rotated natural objects. Psychonomic Bulletin & Review. 2**,** 239-243.
Murray, J. E., 1995b. Negative priming by rotated objects. Psychonomic Bulletin & Review. 2**,** 534-537.
Murray, J. E., 1995c. The role of attention in the shift from orientation-dependent to orientation-invariant identification of disoriented objects. Mem. Cognit. 23**,** 49–58.
Murray, J. E., 1998. Is entry-level recognition viewpoint invariant or viewpoint dependent? Psychonomic Bulletin & Review. 5**,** 300-304.
Nyberg, L., Marklund, P., Persson, J., Cabeza, R., Forkstam, C., Petersson, K. M., Ingvar, M., 2003. Common prefrontal activations during working memory, episodic memory, and semantic memory. Neuropsychologia. 41**,** 371-377.
Otten, L. J., Rugg, M. D., 2001. Task-dependency of the neural correlates of episodic encoding as measured by fMRI. Cereb. Cortex. 11**,** 1150-1160.
Otten, L. J., Rugg, M. D., Interpreting event-related brain potentials. In: T. C. Handy, Ed., Event-related potentials: a methods handbook. vol. The MIT Press, Cambridge, Massachusetts, 2005, pp. 3-16.
Perrin, F., Pernier, J., Bertrand, O., Echallier, J. F., 1988. Spherical splines for scalp potential and current source density mapping. Electroencephalogr. Clin. Neurophysiol. 72**,** 184-187.
Posada, A., Hugues, E., Franck, N., Vianin, P., Kilner, J., 2003. Augmentation of induced visual gamma activity by increased task complexity. Eur. J. Neurosci. 18**,** 2351-2356.
Rainer, G., Miller, E. K., 2000. Effects of visual experience on the representation of objects in the prefrontal cortex. Neuron. 27**,** 179-189.
Schiller, N. O., Münte, T. F., Horemans, I., Jansma, B. M., 2003. The influence of semantic and phonological factors on syntactic decisions: An event-related brain potential study. Psychophysiology. 40**,** 869-877.

Schmitt, B. M., Rodriguez-Fornells, A., Kutas, M., Münte, T. F., 2001. Electrophysiological estimates of semantic and syntactic information access during tacit picture naming and listening to words. Neurosci. Res. 41**,** 293-298.

Singer, W., Gray, C. M., 1995. Visual feature integration and the temporal correlation hypothesis. Annu. Rev. Neurosci. 18**,** 555-586.

Takashima, A., Jensen, O., Oostenveld, R., Maris, E., van de Coevering, M., Fernandez, G., 2006. Successful declarative memory formation is associated with ongoing activity during encoding in a distributed neocortical network related to working memory: A magnetoencephalography study. Neuroscience. 139**,** 291-297.

Tallon-Baudry, C., Bertrand, O., 1999. Oscillatory gamma activity in humans and its role in object representation. TICS. 3**,** 151-162.

Tallon-Baudry, C., Bertrand, O., Delpuech, C., Pernier, J., 1996. Stimulus specifity of phase-locked and non-phase-locked 40 Hz visual response in human. Eur. J. Neurosci. 16**,** 4240-4249.

Tallon-Baudry, C., Bertrand, O., Delpuech, C., Pernier, J., 1997. Oscillatory gamma-band (30-70 Hz) activity induced by a visual search task in human. J. Neurosci. 17**,** 722-734.

Tallon-Baudry, C., Bertrand, O., Henaff, M.-A., Isnard, J., Fischer, C., 2005. Attention modulates gamma-band oscillations differently in the human lateral occipital cortex and fusiform gyrus. Cereb. Cortex. 15**,** 654-662.

Trujillo-Barreto, N. J., Aubert-Vazquez, E., Valdés-Sosa, P. A., 2004. Bayesian Model Averaging in EEG/MEG imaging. NeuroImage. 21**,** 1300-1319.

van Turennout, M., Ellmore, T., Martin, A., 2000. Long-lasting cortical plasticity in the object naming system. Nat. Neurosci. 3**,** 1329-1334.

Varela, F., Lachaux, J. P., Rodriguez, E., Martinerie, J., 2001. The brainweb: Phase synchronization and large-scale integration. Nat. Rev. Neurosci. 2**,** 229-239.

Willems, B., Wagemans, J., 2001. Matching multicomponent objects from different viewpoints: Mental rotation as normalization? J. Exp. Psychol. Hum. Percept. Perform. 27**,** 1090-1115.

Womelsdorf, T., Fries, P., Mitra, P. P., Desimone, R., 2006. Gamma-band synchronization in visual cortex predicts speed of change detection. Nature. 439**,** 733-736.

Worsley, K. J., Marrett, S., Neelin, P., Evans, A. C., 1996. Searching scale space for activation in PET images. Hum Brain Mapp. 4**,** 74-90.

Legends to Figures:

Figure 1. Grand mean baseline corrected ERPs for 0° (black line), 60° (dotted line) and 120° (magenta line) at three regional means: a) anterior, b) occipital and c) parietal, showing the N1 anterior/posterior, P300 and parietal negativity components. Note: different voltage scales.

Figure 2. Grand mean baseline-corrected TF-plots averaged across all three experimental conditions and all electrodes. a) Evoked GBA; b) Induced GBA. Black boxes indicate the time-window of interest (Note: different scales).

Figure 3. Grand mean 3D spherical spline amplitude-maps for evoked (a) and induced (b) gamma-band activity, based on the ±5Hz frequency band centred on the wavelet with maximal activity during the time-window of interest.

Figure 4. Latencies of induced GBA for 0°, ±60° and ±120° conditions. a) Bar Plot of peak latencies' means, with +1 SE bars. b) Box plot of peak latencies' distributions; midlines indicating medians, ends of boxes indicating 25th and 75th percentiles, ends of lines indicating 10th and 90th percentiles and dots indicating observations falling in the outlying 10 percentiles.

Figure 5. Time-course of induced GBA (parieto-occipital regional mean) with the time window for peak analyses indicated by a grey rectangle. a) Grand mean across participants around the central gamma-band wavelet (52.5-57.5 Hz). b) Individual maximal-wavelet activity in the ±5 Hz range around the maximal wavelet for a typical participant (50-60 Hz) (note: different voltage scales).

Figure 6. Source localisation of induced GBA : a) significantly activated areas for upright, ±60° and ±120° conditions; b) areas that showed significant differences in levels of activity between upright and disoriented conditions (subtractions: ±60° and upright; ±120° and upright). Colourbars reflect above threshold T^2 values ($p < 0.01$) (note: different T^2 values across conditions).

Figure 7. Schematic representation of the 128-channel montage. Anterior, parietal and occipital regional means clusters as used for statistical analysis of ERP data are depicted, with indications of extended 10-20 sites approximated to the closest position on the electrode cap.

Figure 1

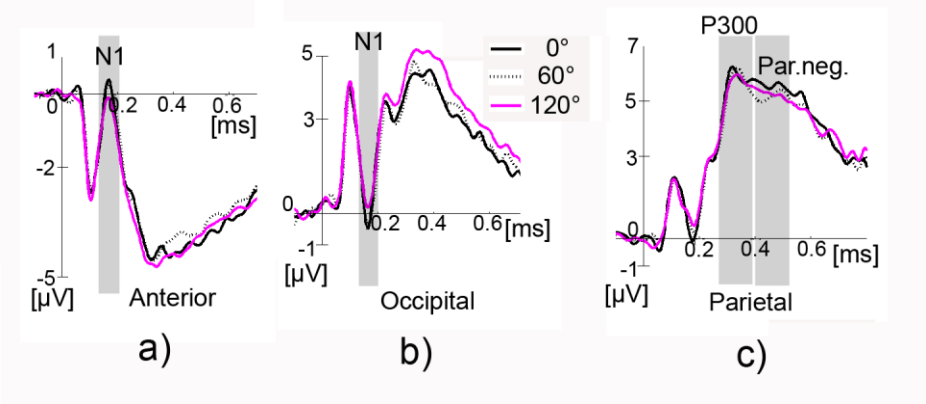
N1
1
0
-2
-5
0.2
0.4
0.6
[ms]
[µV]
Anterior
a)
N1
5
3
0
-1
0.2
0.4
0.6
[ms]
[µV]
Occipital
b)
0°
60°
120°
P300
Par.neg.
7
5
3
0
-1
0.2
0.4
0.6
[ms]
[µV]
Parietal
c)

Figure 2

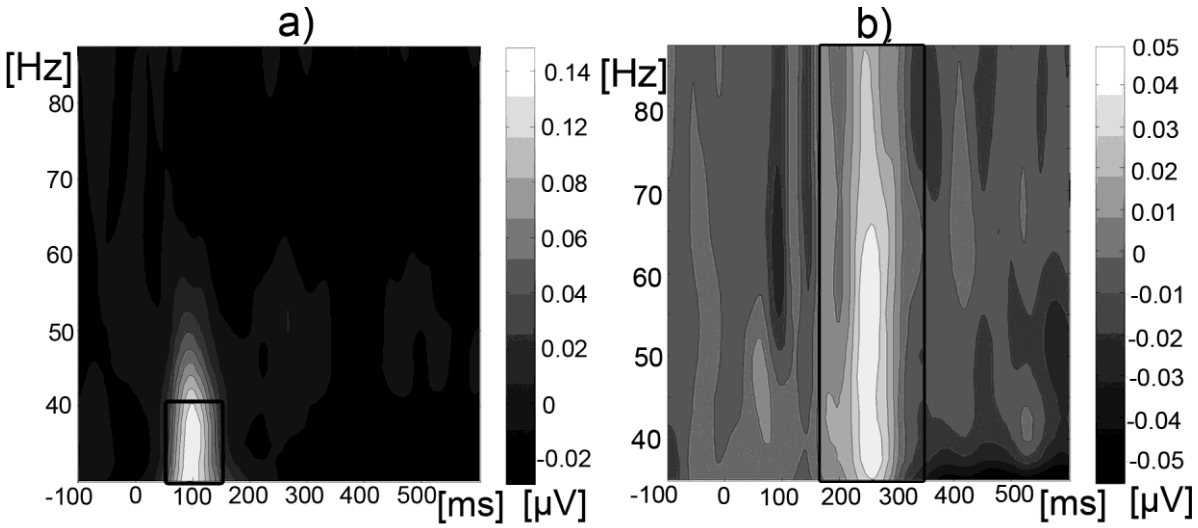
a)
[Hz]
80
70
60
50
40
-100
0
100
200
300
400
500
[ms]
0.14
0.12
0.08
0.06
0.04
0.02
0
-0.02
[μV]
b)
[Hz]
80
70
60
50
40
-100
0
100
200
300
400
500
[ms]
0.05
0.04
0.03
0.02
0.01
0
-0.01
-0.02
-0.03
-0.04
-0.05
[μV]

Figure 3

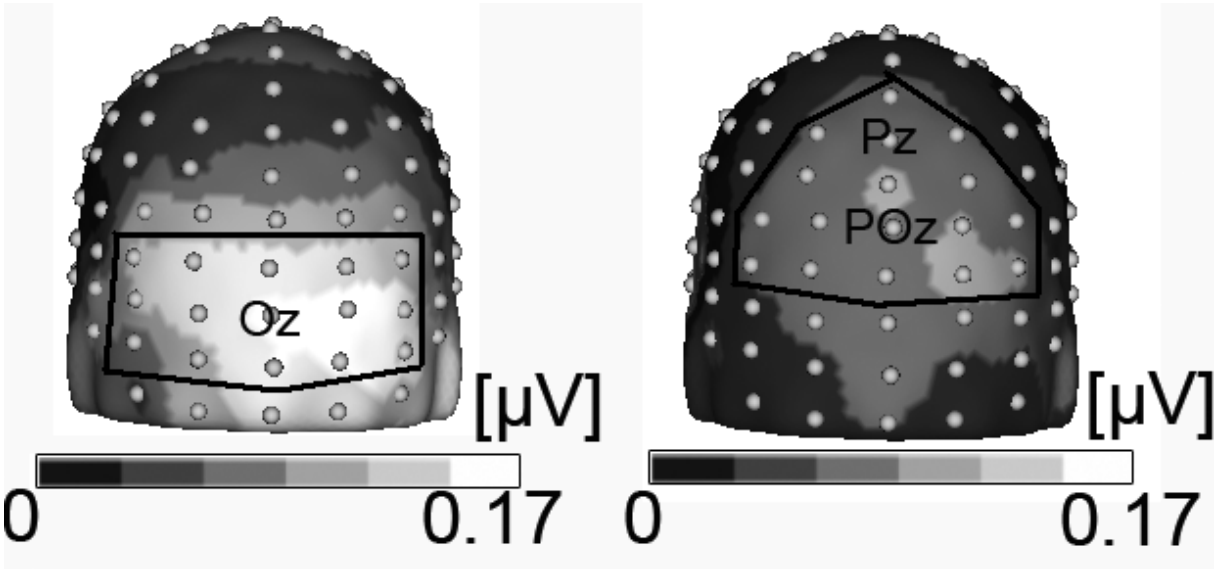

Figure 4

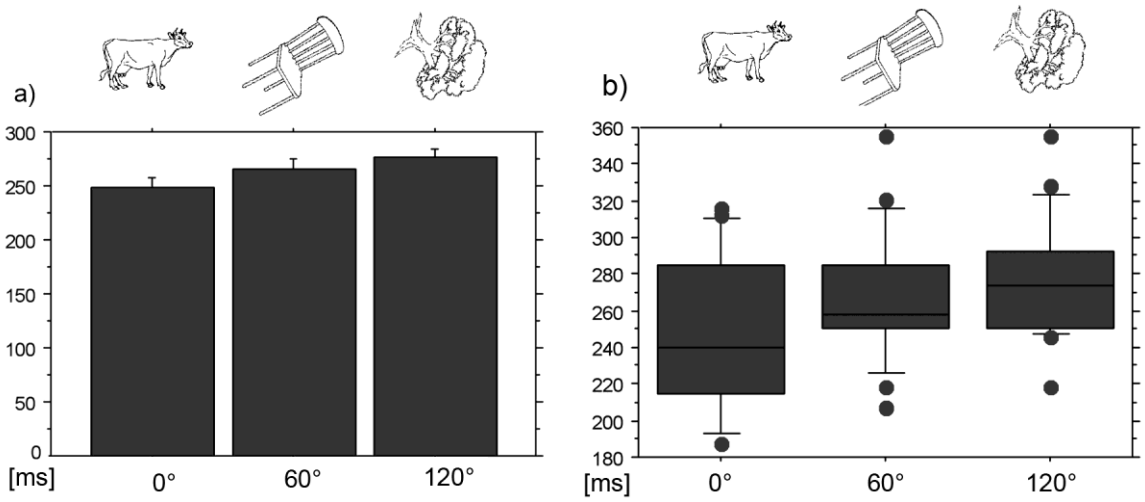
a)
300
250
200
150
100
50
0
[ms]
0°
60°
120°
b)
360
340
320
300
280
260
240
220
200
180
[ms]
0°
60°
120°

Figure 5

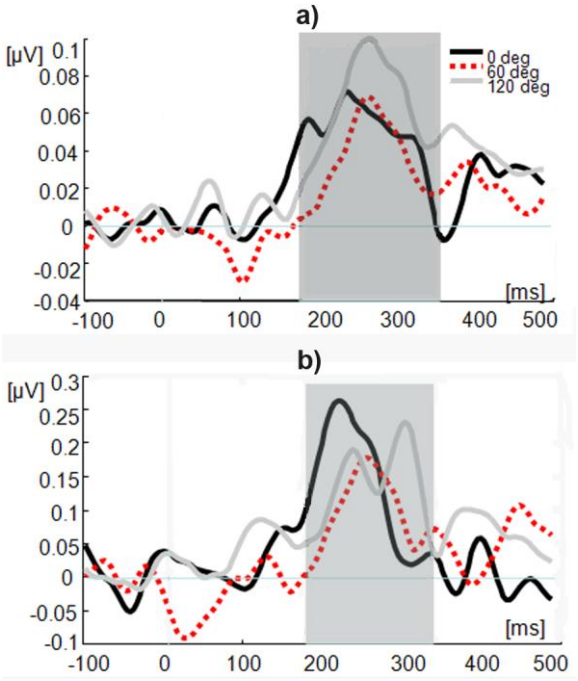
a)
[μV]
0.1
0.08
0.06
0.04
0.02
0
-0.02
-0.04
0 deg
60 deg
120 deg
[ms]
-100
0
100
200
300
400
500
b)
[μV]
0.3
0.25
0.2
0.15
0.1
0.05
0
-0.05
-0.1
[ms]
-100
0
100
200
300
400
500

Figure 6

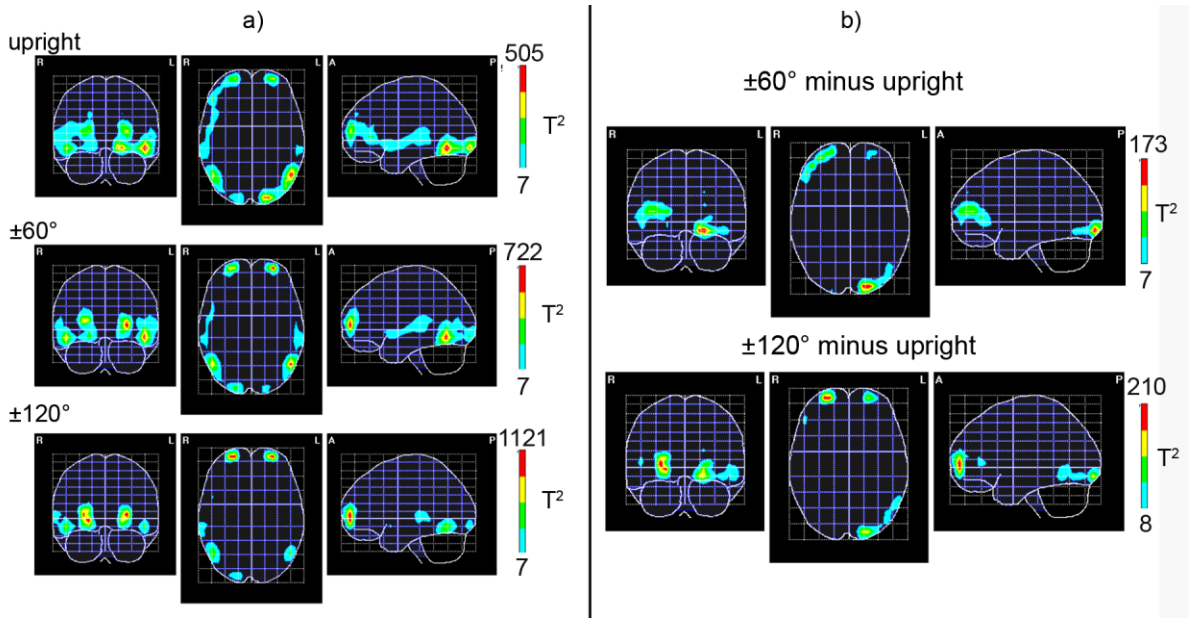
a)
upright
505
T²
7
±60°
722
T²
7
±120°
1121
T²
7
b)
±60° minus upright
173
T²
7
±120° minus upright
210
T²
8

Figure 7

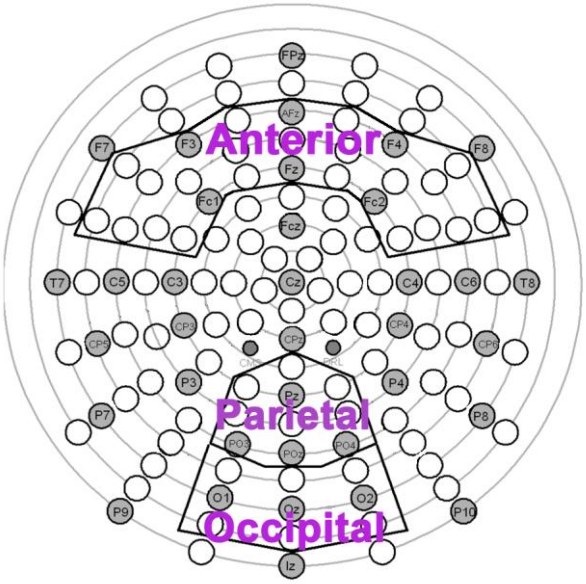
FPz
AFz
F7
F3
Anterior
F4
F8
Fz
Fc1
Fc2
Fcz
T7
C5
C3
Cz
C4
C6
T8
CP5
CP3
CP1
CP2
CP4
CP6
P3
Pz
P4
P7
Parietal
P8
PO3
PO4
O1
Oz
O2
P9
P10
Occipital
Iz

Table 1. Control experiment: accuracy rates and reaction times (mean medians and SEs across subjects in ms) across subjects for overt naming and gender decision tasks (n=12)

	Orientation					
	0°		**± 60°**		**± 120°**	
	RT	% correct	RT	% correct	RT	% correct
Overt	886	77.0	947	78.2	946	70.8
naming	(21)	(2.0)	(25)	(3.0)	(31)	(4.2)
Gender	1164	82.7	1202	77.5	1284	75.1
decision	(28)	(2.8)	(34)	(3.2)	(39)	(4.5)

Table 2. ERPs: definitions of components with mean baseline corrected amplitudes and F-values for all three conditions (n=18)

Component	**Site**	**Time window (ms)**	**µV (Mean ± SE)**			**F-value (p-value)**
			0°	**60°**	**120°**	
N1 anterior	Anterior	145-195	-0.13 ± 0.37	-0.16 ± 0.41	-0.41 ± 0.38	2.28 (0.12)
N1 posterior	Occipital	145-195	0.23 ± 0.58	0.24 ± 0.57	0.57 ± 0.59	1.66 (0.20)
P300	Parietal	280-400	3.89 ± 0.59	3.82 ± 0.47	4.14 ± 0.53	1.13 (0.33)
Parietal negativity	Parietal	400-500	3.64 ± 0.50	3.52 ± 0.45	3.88 ± 0.57	1.20 (0.31)

Table 3. GBA: mean peak amplitudes and latencies with standard errors and F-values

		Condition			**F-value**
		0°	**±60°**	**±120°**	**(2,17)**
Induced GBA	Mean peak amplitude [μV]	0.07 ± 0.01	0.07 ± 0.02	0.08 ± 0.01	0.76, n.s.
	Mean peak latency [ms]	248 ± 10	266 ± 8	276 ± 8	3.48, $p<0.05$
Evoked GBA	Mean peak amplitude [μV]	0.14 ± 0.04	0.13 ± 0.03	0.15 ± 0.04	0.12, n.s.
	Mean peak latency [ms]	106 ± 5	100 ± 5	106 ± 6	0.38, n.s.

Table 4. Induced GBA: Montreal Neuroscience Institute coordinates of all significantly activated sources (X, Y, Z; in order of decreasing magnitude) and a brief anatomical description of relevant brain areas.

		x, y, z	**Anatomical description**
Conditions	*upright*	-50 -62 -10	lateral occipitotemporal gyrus left
		-18 -91 -10	lingual gyrus left
		51 -62 -10	inferior temporal gyrus right
		-25 62 12	middle frontal gytrus left
		23 62 12	middle frontal gyrus right
	±60°	-28 60 5	middle frontal gyrus left
		-50 -63 -10	lateral occipitotemporal gyrus left
		26 60 12	middle frontal gyrus right
		50 -62 -10	inferior temporal gyrus right
	±120°	23 62 -2	middle frontal gyrus right
		-28 61 5	middle frontal gyrus left
		50 -63 -10	inferior temporal gyrus right
		-50 -61 -10	lateral occipitotemporal gyrus left
Subtractions	*±120°*	28 62 5	middle frontal gyrus right
	vs.	-16 -91 -10	lingual gyrus left / occipital pole left
	upright	-21 62 -2	middle frontal gyrus left
		-44 -74 -10	lateral occipitotemporal gyrus left
		-55 -55 -10	middle temporal gyrus left
	±60°	-18 -91 -10	lingual gyrus left
	vs.	35 54 12	middle frontal gyrus right
	upright	-28 61 5	middle frontal gyrus left
		-28 -91 -10	lateral occipitotemporal gyrus left